Ionic liquid/poly(ionic liquid) membranes as non-flowing, conductive materials for electrochemical gas sensing

Authors

Simon Doblinger,[1] Catherine E. Hay,[1] Liliana C. Tomé,[2] David Mecerreyes,[3,4] Debbie S. Silvester[1,*]

Affiliations

[1] School of Molecular and Life Sciences, Curtin University, GPOBox U1987, Perth 6845, Western Australia, Australia;

[2] LAQV-REQUIMTE, Department of Chemistry, NOVA School of Science and Technology, FCT NOVA, Universidade Nova de Lisboa, 2829-516 Caparica, Portugal;

[3] POLYMAT University of the Basque Country UPV/EHU, 20018 Donostia-San Sebastian, Spain;

[4] IKERBASQUE, Basque Foundation for Science, 48013 Bilbao, Spain

*corresponding author: d.silvester-dean@curtin.edu.au

Abstract

Ionic liquids (ILs) are highly promising, tuneable materials that have the potential to replace volatile electrolytes in amperometric gas sensors in a 'membrane-free' sensor design. However, the drawback of removing the membrane is that the liquid ILs can readily leak or flow from the sensor device when moved/agitated in different orientations. A strategy to overcome the flowing nature of ILs is to mix them with polymers to stabilise them on the surface in the form of membranes. In this research, the poly(ionic liquid) (poly(IL), poly(diallyldimethylammonium bis(trifluoromethylsulfonyl)imide), poly[DADMA][NTf_2]) has been mixed with a common room temperature ionic liquid, 1-ethyl-3-methylimidazolium bis(trifluoro-methylsulfonyl)imide ([C_2mim][NTf_2]) to form stable membranes on miniaturised, planar electrode devices. Different mixing ratios of the IL/poly(IL) have been explored to find the optimum membrane that gives both high robustness (non-flowing material) and adequate conductivity for measuring redox currents, with the IL/poly(IL) 60/40 wt.% proving to give the best responses. After assessing the blank potential windows on both platinum and gold electrodes, followed by the kinetics of the cobaltocenium/cobaltocene redox couple, the voltammetry of oxygen, sulfur dioxide and ammonia gases have been studied. Not only were the membranes highly robust and non-flowing, but the analytical responses towards the gases were excellent and highly reproducible. The presence of the poly(IL) negatively affected the sensitivity, however the electron transfer kinetics and the limit of detection were actually improved for O_2 and SO_2, combined with the poly(IL) experiencing less reference potential shifting. These promising results show that membranes containing conductive poly(IL)s mixed with ionic liquids could be used as new 'designer' gas sensor materials in robust membrane free amperometric gas sensor devices.

Keywords: *ionic liquids, poly(ionic liquid)s, gas sensing, voltammetry, oxygen, sulfur dioxide, ammonia,*

1. Introduction

Amperometric gas sensors (AGSs) are important devices that are used to quickly quantify a gaseous substance based on measuring the current response at a potential where the gas is redox active [1-3]. Commercially available AGSs are typically based on the historical Clark type design [4], composed of two (or three) electrodes, connected through an electrolyte/solvent system (usually water/sulfuric acid) and covered with a gas permeable membrane. The role of the membrane is to retain the solvent inside the sensor, in addition to imparting some selectivity towards different gases like oxygen (O_2), carbon dioxide (CO_2), sulfur dioxide (SO_2) or ammonia (NH_3). Limitations of traditional AGSs include both the evaporation and solidification of the solvent at high or low temperatures, and the long response times caused by slow diffusion of gas through the membrane. Employing room temperature ionic liquids (RTILs) as alternative solvents in AGSs may overcome some of these drawbacks [3]. RTILs are being considered as replacements for conventional electrolyte/solvent systems in electrochemistry due to their promising characteristics, such as high conductivity, wide electrochemical windows, high chemical and thermal stability and good solubilisation properties [5]. They exist in the liquid state over a wide temperature range and have negligible vapour pressures, therefore they do not evaporate and can be used in a 'membrane-free' AGS design [3, 6-9]. However, the flowing nature of the RTIL electrolyte prevents the planar 'membrane-free' style sensors from being robust enough for applications, meaning the liquid must be encapsulated because it will leak if the sensor is used in different orientations.

One way to make liquid electrolytes more robust is to solidify them by the addition of polymers. Lee et al. used a gel-polymer electrolyte containing common polymers mixed with RTILs for oxygen sensing on low-cost planar electrodes [10]. Adding 50 wt.% of poly(methyl methacrylate) (PMMA) to pure 1-ethyl-3-methylimidzolium bis(trifluoromethylsulfonyl)imide ($[C_2mim][NTf_2]$) resulted in an electrolyte that did not flow, but was still conductive enough to be used for oxygen sensing [10]. This proof-of-principle study showed that the device could successfully be used to detect oxygen in various orientations without change in the current response, whereas the response was significantly changed using the pure RTIL. Other polymers that have been mixed with ionic liquids and used for gas and humidity sensing in ionic liquids include: poly(vinylidene fluoride-co-hexafluoropropylene) [11], poly(vinylidene fluoride) [12] and poly(ethylene glycol) methyl ether methacrylate [13].

Poly(ionic liquid)s, abbreviated in this work as poly(IL)s, are polyelectrolyte materials that combine the promising characteristics of pure ILs with the physical stability of polymers [14]. They have drawn increasing attention in various fields over the last decade [14]. For example, in the healthcare sector, Qin et al. [15] used pyrrolidinium-based poly(IL) membranes as eco-friendly and antibacterial materials with low cytotoxicity towards human cells. In materials science, PEDOT (poly(3,4-ethylenedioxythiophene)/poly(IL) dispersions were explored in organic light emitting diodes (OLEDs) as superior and more stable alternatives to aqueous PEDOT/PSS (poly(styrene sulfonate sodium salt)) electrolytes, which degrade over time due to the presence of water and acidic PSS [16, 17]. A review by Zhang et al. [18] described various applications of poly(IL)-composites, such as gold nanoparticle-porous imidazolium poly(IL)s as microfluidic reactors with high

conversion activity and selectivity for the reduction of nitrobenzene derivatives [19], and poly(IL)-metal salt composites as solid electrolytes in batteries [20]. A highly active research area involves the use of poly(IL)s as materials for efficient gas sorption [21], gas separation membranes [22] and in flexible electronics [23]. The most detailed studied gas so far is carbon dioxide due to the CO_2-affinity of ILs. Different strategies for the fabrication of these membranes have been investigated, including neat poly(IL) membranes [24], co-polymer membranes [25], and IL/poly(IL) membranes [26], and they have also been used for CO_2 conversion to cyclic carbonates [27]. In particular, the incorporation of ILs into poly(IL)s is driven by the desire to combine the high gas permeability of ILs and the mechanical stability of polymers in order to enhance the membrane performance. Because IL/poly(IL) composites have been used as quasi-solid electrolytes [20], as well as high performance membranes for gas separation [26], this makes them promising candidates for gas sensing applications.

Poly(IL)-based sensors for pH [28], ions [29], biomolecules [30] and gases [31, 32] have been explored by different groups. Willa et al. [31] incorporated $La_2O_2CO_3$ in membranes to detect CO_2 by electrochemical impedance spectroscopy which resulted in good sensitivity in humid environments. Ji et al. [32] combined poly(IL)s with single walled carbon nanotubes for CO_2 sensing via impedance spectroscopy, which resulted in good selectivity. However, UV irradiation was required to desorb the gas for reproducibility.

Despite their promising properties, the use of poly(IL)s as robust electrolytes in amperometric gas sensors has not yet been explored so far. Therefore, in this work, we demonstrate for the first time that IL/poly(IL) membranes can be used as highly favourable and robust electrochemical solvents for amperometric gas sensing applications. The fundamental electrochemical behaviour of these new materials is first examined by studying the electrochemical window response and the redox behaviour of the solid bis(cyclopentadienyl)cobalt(III) hexafluorophosphate. Then, the applicability of the IL/poly(IL) membranes to act as electrolytes for gases is demonstrated in both the cathodic and anodic regions by studying the reduction of oxygen (O_2), the reduction of sulfur dioxide (SO_2), and the oxidation of ammonia (NH_3). It will be shown that these materials are not only highly robust, but they give highly reproducible current responses, with less reference potential shifting and fewer voltammetric impurities in the cathodic region compared to the pure IL, allowing the possibility to detect lower analyte concentrations in the future.

2. Experimental

2.1 Chemical Reagents

The RTIL 1-ethyl-3-methylimidazolium bis(trifluoromethylsulfonyl)imide ([C_2mim][NTf_2], 99.5%, IoLiTec-Ionic Liquids Technologies GmbH, Heilbronn, Germany) was purchased at the highest purity possible and used as received. The poly(ionic liquid) (poly(IL)) poly(diallyldimethylammonium bis(trifluoromethyl-sulfonyl)imide) (poly[DADMA][NTf_2]) was synthesised by an anion metathesis from the poly(diallyldimethylammonium chloride) precursor (average MW 400,000 and 500,000, 20 wt.% in water, Sigma Aldrich), according to established procedures [33]. Acetone (CHROMASOLV®, for HPLC, ≥99.0%, Sigma-Aldrich) was used as received. A 0.5 M solution of H_2SO_4(aq) was prepared by diluting a 95-98 wt.% H_2SO_4 solution (Ajax Finechem, WA, Australia) with ultrapure water and used for activation of the thin-film electrodes. Sulfur dioxide (509 ppm in nitrogen), ammonia (969 ppm in nitrogen) and oxygen (99.99%, high purity) gas cylinders were purchased from Coregas (NSW, Australia) and high purity nitrogen (99.999 %) was purchased from BOC Gases (Welshpool, WA, Australia). Bis(cyclopentadienyl)cobalt(III) hexafluorophosphate ([$Co(C_5H_5)_2$]PF_6 or $CcPF_6$, 98%, Sigma-Aldrich) was used as received.

2.2 IL/poly(IL) Membrane Preparation

Different ratios of IL/poly(IL) in the mixture were prepared according to the masses given in Tables S1 and S2 in the supporting information. The poly(IL) (solid) was weighed directly into a glass vial and dissolved in the respective amount of acetone. The appropriate mass of IL was then added, and the mixture was capped and stirred overnight at room temperature using a magnetic stirrer at a rotation speed of ~400 rpm. Ca. 19 µL of the mixture was drop casted onto the planar thin-film electrode and the casting solvent was left to evaporate slowly at room temperature, which was achieved by placing the electrode in a small plastic bag to maintain an atmosphere of acetone. It is noted that the dried film resulted in a free-standing membrane that could be peeled from the electrode if necessary, although peeling was not explored in this work. Figure 1 shows an image of a prepared, peeled film, together with the chemical composition and chemical structures of the poly(IL) and IL studied in this work. We plan to investigate different combinations of ILs and poly(ILs) in membranes and optimise them for gas sensing experiments in the future.

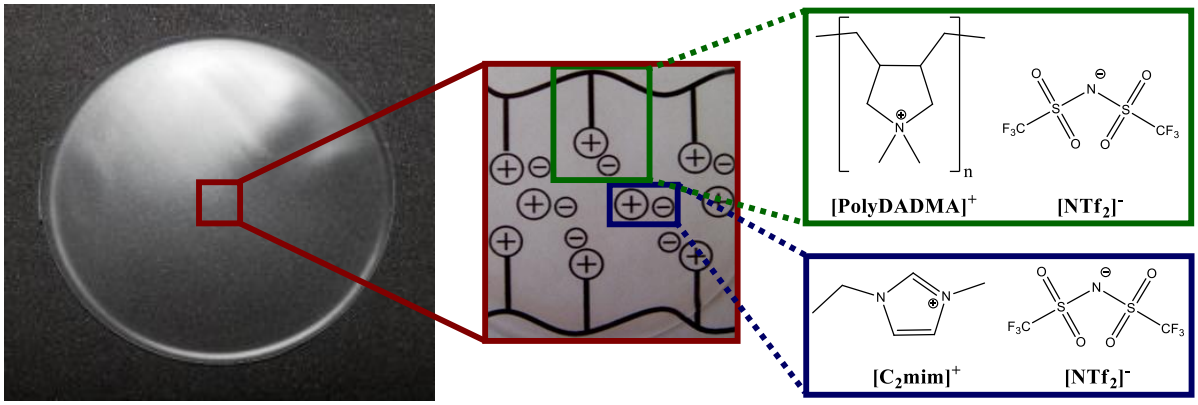

Figure 1. Photo of a circular IL/poly(IL) 60/40 wt.% membrane composed of poly[DADMA][NTf_2] and [C_2mim][NTf_2], which was used as an electrolyte for the electrochemical sensing experiments.

2.3 Electrochemical Experiments

All experiments were performed with a PGSTAT101 Autolab potentiostat (Metrohm Autolab, Gladesville, NSW, Australia) interfaced to a computer with NOVA 1.11 software. The electrochemical cell was housed inside an aluminium Faraday cage to reduce electromagnetic interferences. The working electrode (WE), counter electrode (CE) and reference electrode (RE) of the platinum and gold thin-film electrodes (Pt- and Au-TFEs) (ED-SE1, MicruX Technologies, Oviedo, Spain) were composed of either platinum or gold deposited on a Pyrex substrate, with a WE disk diameter of 1 mm and an in-built CE and RE. An electrode adapter supplied by MicruX was employed to connect the electrodes to the potentiostat. The Pt- or Au-WEs were electrochemically activated prior to each experiment by cyclic voltammetry (CV) cycling between -0.75 and +0.7 V (~100 times at 1 V s^{-1}) in nitrogen purged 0.5 M H_2SO_4(aq) for platinum, and between -0.8 and 1.1 V for gold. The activated chips were then rinsed twice with ultrapure water and acetone before drying under a stream of nitrogen.

For electrochemical sensing experiments, ~7 µL of the pure IL or ~19 µL of the IL/poly(IL) mixture was drop-casted to cover all three electrodes of the TFE, and the casting solvent was evaporated slowly in a closed environment. The cell was then purged for approximately 30 min under a dry nitrogen stream at a flow rate of 500 mL min^{-1} to remove dissolved gases and impurities such as water, oxygen and carbon dioxide. For gas sensing experiments, removal of impurities was monitored by repeated CV scanning until a stable blank response was observed. The gas sensing experiments were purposely performed in a dry environment with <1 % relative humidity, so that the work can be focussed on (a) the effect of changing the membrane composition and (b) changing the nature of the gas, without any additional complications of water present in the system.

For all measurements, the integrated CE and RE (made from the same material as the WE) were used. After obtaining a constant blank, the analyte gas was introduced into one arm of the T-cell. To obtain different concentrations, the analyte gas stream was diluted with nitrogen through a gas mixing system by adjusting the relative gas flow rates [34]. For the cobaltocenium experiments, the pure IL (5 µL) or the respective amount of IL/poly(IL) mixture (~19 µL) was drop-casted onto the TFE to cover all the electrodes and the acetone was evaporated slowly. The cell was purged for approximately 30 min in nitrogen at a flow rate of 500 mL min^{-1} before electrochemical experiments were performed. N_2 flow was maintained throughout the experiments with $CcPF_6$.

3. Results and Discussion

3.1 Electrochemical Window of Membranes

To assess the suitability of different IL/poly(IL) mixtures to act as electrochemical solvents, the potential window of the IL/poly(IL) membranes with different mixing ratios was first explored. Figure 2 shows cyclic voltammetry (CV) on: (a) a platinum thin-film electrode (Pt-TFE), and (b) a gold thin-film electrode (Au-TFE), for the electrochemical windows of three IL/poly(ionic liquid) membranes with ratios of 60/40, 40/60 and 20/80 wt.%, together with the pure IL. Both platinum and gold thin-film electrodes were examined because these are two of the most commonly used surfaces in planar electrode devices for electrochemical sensing experiments in ILs [8], and the potential windows in ILs are known to be influenced by the electrode material [35]. The potential was scanned from 0 V vs the inbuilt pseudo reference, initially in the positive direction until the current reached a "cut-off" current of 10 µA, before being reversed and scanned in the negative direction until reaching a cut-off current of -10 µA, and then scanned back to 0 V to complete a full cycle. By fixing the cut-off currents at the same value, this can approximately account for any potential shifting due to the unstable reference electrode, allowing the focus to be on the width of the potential window and the presence of any redox features in the blank voltammetry.

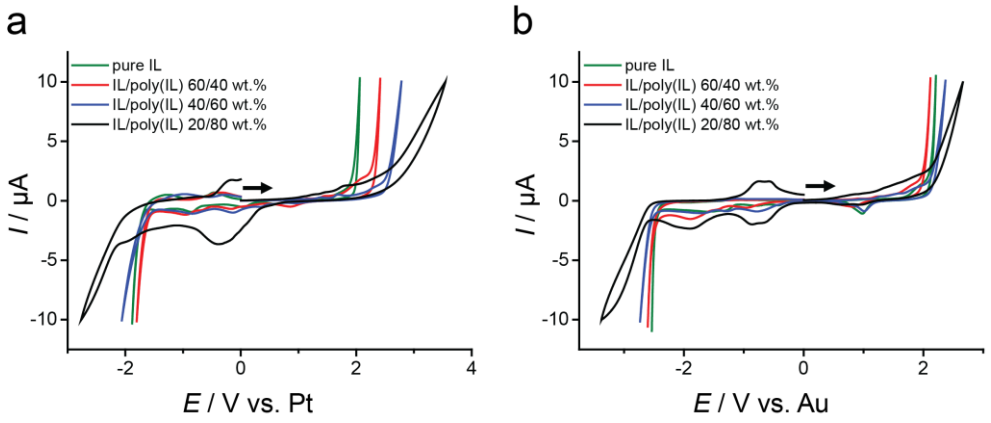

Figure 2. Electrochemical windows of the pure IL and IL/poly(IL) membranes with ratios of 60/40, 40/60 and 20/80 wt.% with a cut-off current of 10 µA on a 1 mm diameter platinum thin-film electrode (a) and a 1 mm diameter gold thin-film electrode (b). All scans were taken at 100 mV s^{-1}. The black arrows indicate the start potential and scan direction.

As seen in Figure 2, in the cathodic region below 0 V, there are some small redox peaks present in the pure IL which are most likely caused by intrinsic dissolved impurities (e.g. unreacted imidazole from the synthesis), as we have discussed in detail in our previous study [35]. The available potential window for the pure [C_2mim][NTf_2] IL (green line) is consistent with the literature [35], with an approximate potential window of up to 4 V (depending on the exact cut-off current chosen). When the IL is incorporated into the poly[DADMA][NTf_2], the potential window becomes slightly wider with increasing poly(IL) content, as observed by the red and blue curves in Figure 2a. It is likely that this is caused by the addition of the poly[DADMA]$^+$ (pyrrolidinium) cation, which is more electrochemically stable compared to the imidazolium cation used in the pure IL [5]. The enhancement in electrochemical window is slightly more prominent on the Pt electrode (Figure 2a) compared to the Au electrode (Figure 2b). On both the Pt-TFE and the Au-TFE, the IL/poly(IL) membrane with 20/80 wt.% ratio (black curve) shows a heavily slanted electrochemical response

at the oxidation and reduction limits, as well as significant redox peaks within the scanned range. The slanted response is not unexpected given the very high polymer content of the mixture and its resulting high viscosity that results in large ohmic drop contributions. Therefore, the IL/poly(IL) membrane with 20 wt.% of IL incorporated, was excluded in our further studies.

For the other two IL/poly(IL) mixtures, the blank voltammograms show sharply increasing oxidation and reduction currents at the potential limits, without significant visible ohmic drop behaviour (slanted voltammetry), which is highly encouraging for their use as electrolytes for sensing applications. It is important to note that these are solid free-standing and flexible films that are strongly mechanically stable on the electrode, making them useful for robust membrane-free sensors without any leakage of the electrolyte. We believe that the high ionic content of the poly(IL) (polymerised cation and freely mobile counter anion) provides good conductivity of the membranes, so they retain promising electrochemical characteristics, even when they are solid materials. Conductivities of similar membrane mixtures (but with the *N*-methyl-*N*-butylpyrrolidinium IL cation, compared to the 1-ethyl-3-methylimidazolium cation used in the current work) have been reported previously, and reveal a roughly one order of magnitude decrease in conductivity of the pure IL when mixed with the poly(IL) at a 50:50 % weight ratio [36].

3.2 Behaviour of the Dissolved Solid Cobaltocenium Hexafluorophosphate

Before employing the IL/poly(IL) membranes for gas sensing, the electrochemical behaviour of a conventional "ideal" redox species in the membrane was first studied to observe the effect on the both the current response and redox kinetics as the polymer content is increased. Cobaltocenium hexafluorophosphate has been reported to be an ideal redox species in aprotic solvents and ionic liquids [37], and was chosen over ferrocene due to the moderate volatility of ferrocene from ionic liquids [38], which would change the current response. The electrochemical reduction of cobaltocenium hexafluorophosphate ($[Co(C_5H_5)_2]PF_6$) in ILs proceeds by a reversible one electron reaction according to equation 1 [37].

$$[Co(C_5H_5)_2]^+ + e^- \rightleftharpoons [Co(C_5H_5)_2] \quad (1)$$

For simplicity, the bis(cyclopentadienyl)cobalt(III) complex ($[Co(C_5H_5)_2]^+$) will be abbreviated as Cc^+ in the following discussion. Figure 3 shows cyclic voltammetry for the reduction of $CcPF_6$ in pure $[C_2mim][NTf_2]$ IL and the IL/poly(IL) membranes containing 40 and 60 wt.% of IL on gold thin-film electrodes (Au-TFEs) at a scan rate of 100 mV s^{-1}. One main reduction peak and its corresponding oxidation peak were observed in all samples, with a small pre-peak that is present in the blank IL (see discussion on impurities in the previous section). Smaller currents for the Cc^+/Cc redox process at ~-1.3 V were observed as the poly(IL) content increased, which is to be expected because of the higher viscosity and therefore reduced diffusion coefficient of Cc^+. It is noted that the amount of Cc^+ used in all mixtures was fixed at 0.025 wt.% (rather than using a concentration in millimolar) to account for the presence of both solid (polymer) and liquid (IL) components of the membrane, and noting that the solid Cc^+ analyte is not expected to dissolve in the solid poly(IL) regions.

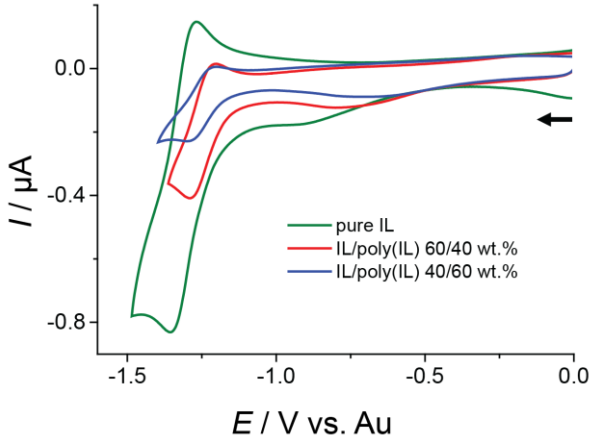

Figure 3: Cyclic voltammetry (CV) for the electrochemical reduction of 0.025 wt.% $CcPF_6$ in the pure IL, IL/poly(IL) membranes with 60 and 40 wt.% of IL incorporated on a Au-TFE (diameter =1 mm). The scans were performed at 100 mV s^{-1} under a nitrogen flow of 500 mL min^{-1}.

The currents and peak-to-peak separations, ΔE_p, for the Cc^+/Cc redox couple from the CVs in Figure 3 are shown in Table 1. The currents decrease systematically as the poly(IL) content is increased, as expected because the membrane becomes increasingly viscous. ΔE_p increases systematically as more poly(IL) is added to the mixture, likely because the more viscous membrane gives rise to higher resistance and some increased ohmic drop contributions. The kinetics of the Cc^+/Cc redox couple are not typically an ideal fast (56 mV) electron transfer process in ILs anyway, because the high viscosity slows ion dynamics and reduces heterogeneous electron transfer rate constants in ILs [39], so the ΔE_p values obtained here for the pure IL are quite consistent with those reported in the literature [40]. Plots of peak current *vs* the square root of the scan rate (scan rates of 10 to 1000 mVs^{-1}) were linear (see supporting information Figure S1), suggesting that the process is diffusion controlled both within the pure IL and the in the membranes.

Table 1: Comparison of peak current (I) and peak-to-peak separation (ΔE_p) of the Cc^+/Cc redox couple (at 0.025 wt.% $CcPF_6$) in pure [C_2mim][NTf_2] and IL/poly(IL) membranes of different compositions.

Electrolyte	$-I$ / µA	ΔE_p / mV
Pure IL	0.83	76
IL/poly(IL) 60/40 wt.%	0.41	88
IL/poly(IL) 40/60 wt.%	0.23	98

3.3 Gases

To demonstrate the suitability of the different IL/poly(IL) membranes to act as electrolytes for gas detection, oxygen, sulfur dioxide and ammonia were chosen as target gases. Different concentrations of the gases were introduced to the environment above the membrane, and using cyclic voltammetry, calibration graphs can be produced, and analytical parameters such as sensitivity and limit of detection can be calculated. The three gases have been studied in ILs previously by our group [10, 41, 42], and were chosen because they exhibit redox behaviour in both the cathodic and anodic regions of the potential window, allowing for the assessment of IL/poly(IL) membranes as electrolytes over a wide range of potentials. In the amperometric gas sensor design used in this work, the gas must first partition into the IL/poly(IL) membrane, before diffusing to the electrode where it is oxidised or reduced, producing a current response.

3.3.1 Oxygen

The electrochemical oxygen reduction reaction (ORR) in aprotic ILs has been studied [43] and is known to undergo an electrochemically quasi-reversible one electron reduction according to equation 2.

$$O_2 + e^- \rightleftharpoons O_2^{\bullet -} \quad (2)$$

Figure 4 shows the electrochemical response for the reduction of oxygen at concentrations from 0 – 100 vol.% O_2 on a platinum thin-film electrode (Pt-TFE) at a scan rate of 100 mV s^{-1} in (a) pure [C_2mim][NTf_2], and different ratios of [C_2mim][NTf_2]/poly(IL) mixtures: (b) 60/40 wt.% and (c) 40/60 wt.%. The blank measurements in the absence of oxygen are shown as dashed lines. All three membrane compositions show chemically reversible responses, indicating that the superoxide ion is stable on the electrochemical timescale. Plots of peak current vs the square root of scan rate are linear (see Figure S2), suggesting that the oxygen process is diffusion controlled in both the pure IL and in the membranes. Excellent analytical responses are also observed, where the currents increase linearly with increasing oxygen concentration (R^2 > 0.999). Reproducibility is also excellent between devices on repeat calibration runs (<5 % variation in current), as evidenced by the very small error bars in the calibration graphs. This suggests a high quality working electrode surface with a stable electroactive surface area, provided the pre-cleaning protocols are followed.

Calibration plots of peak current vs concentration, along with the corresponding lines of best fit, are shown together in Figure 4d (and the slope/sensitivity is given in Table 2) for all three electrolyte compositions. The sensitivities of the calibration graphs decrease with increasing polymer content in the electrolyte, as expected due to the increase in viscosity of the electrolyte. It is noted that the solubility of oxygen (and other gases) may also change with increasing polymer content, which may also affect the current response; measuring gas solubilities in these electrolytes will be a focus of our future research.

Interestingly, despite the electrolyte changing from a liquid to a IL/poly(IL) membrane, there is no obvious difference in the peak shape and peak-to-peak separation for the oxygen/superoxide redox couple that would suggest more resistive behaviour. This is in contrast with our previous work in PMMA/IL mixtures, where the 50:50 mixture PMMA/IL film was very resistive and showed highly slanted responses for oxygen reduction [10]. In fact, not only do the peak shapes in Figure 5 not appear to visually change (by eye), the kinetics of the redox process actually become *faster* (smaller peak-to-peak separation) upon the polymer addition. Table 2 shows the ΔE_p values, which are more than 80 mV smaller in the IL/poly(IL) membranes compared to the pure IL; this is highly beneficial for robust oxygen sensing in the IL/poly(IL) materials. The reason for the reduction in ΔE_p is likely to be because of the faster oxygen/superoxide kinetics with the pyrrolidinium moiety compared to the imidazolium moiety.

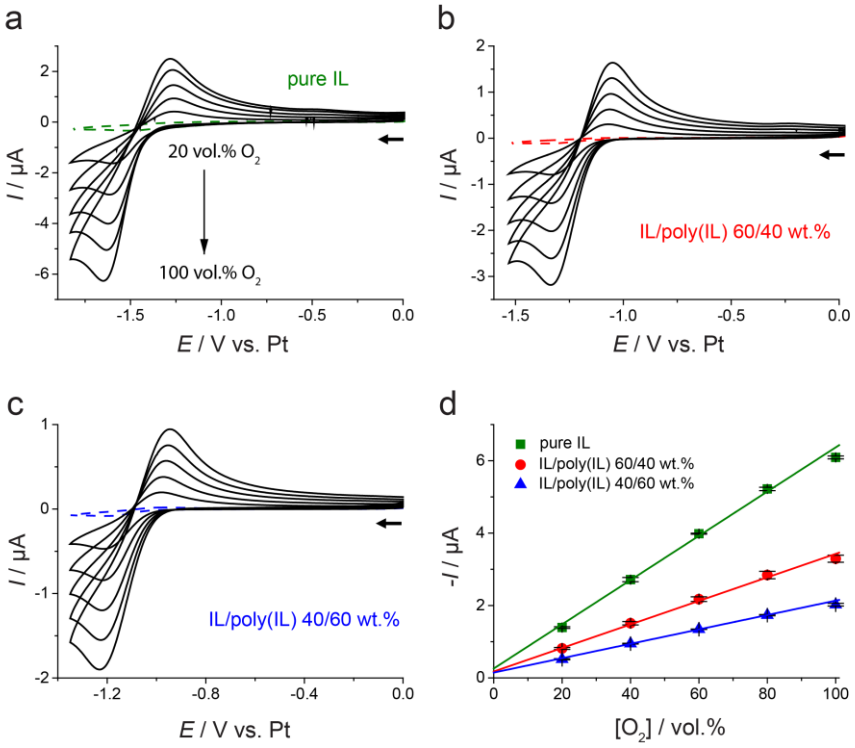

Figure 4. Cyclic voltammetry for electrochemical oxygen reduction at concentrations between 20 and 100 vol.% in (a) pure IL, (b) IL/poly(IL) 60/40 wt.% (c)) IL/poly(IL) 40/60 wt.% and (d) the respective baseline corrected calibration curves on a Pt-TFE (diameter = 1 mm). The dashed line represents the blank without O_2 at a scan rate of 100 mV s^{-1} and an overall flow rate of 500 mL min^{-1}. Error bars in (d) show one standard deviation for three runs on separate electrode devices.

The limit of detection (LOD) was calculated from the calibration graphs (using three standard deviations of the calibration line) and is shown in Table 2 for all three samples. The LOD values are actually observed to slightly *improve* with higher poly(IL) content, revealing that even though the sensitivities are negatively affected by the higher film viscosity, the limit of detection is not. We believe this is because of the higher R^2 value of the calibration line obtained for the membranes (see table 2) as a result of the slightly cleaner blank responses with less impurities (dashed lines in Figure 4) as more polymer is added. Because poly(IL)s are solid materials, they are easier to purify post-synthesis via re-crystallisation compared to the ILs. This is a benefit for sensing applications because it could help to detect lower concentrations of gases that are redox active in the potential range where intrinsic impurity peaks are present.

Table 2. Summary of analytical parameters obtained for gases in the cathodic region (oxygen and sulfur dioxide): Pearson correlation coefficient R^2, sensitivity, calculated limit of detection (LOD), and peak-to-peak separation ΔE_p for the highest gas concentration for the electrochemical oxygen reduction, and sulfur dioxide reduction in the pure IL and IL/poly(IL) membranes.

	Oxygen				Sulfur Dioxide			
Sample	R^2	Sensitivity / nA/vol.%	LOD / vol.%	ΔE_p / mV	R^2	Sensitivity / nA/ppm	LOD / ppm	ΔE_p / mV
Pure IL	0.9996	-61 ± 3	8.8 ± 0.4	369	0.9993	-3.83 ± 0.05	21 ± 5	137
IL/poly(IL) 60/40 wt.%	0.9999	-33 ± 1	9.0 ± 0.8	286	0.9997	-2.10 ± 0.01	20 ± 4	142
IL/poly(IL) 40/60 wt.%	0.9999	-20 ± 1	8.3 ± 1.2	286	0.9995	-1.15 ± 0.06	18 ± 4	134

3.3.2 Sulfur Dioxide

The electrochemical mechanism for the reduction of sulfur dioxide has been studied previously by various researchers [41, 44], and is believed to follow equations (3) to (8), involving a one-electron reduction of SO_2 to the radical, which can undergo different chemical transformations, and several oxidation processes on the reverse sweep:

$$SO_2 + e^- \rightleftharpoons SO_2^{\bullet -} \quad (3)$$

$$SO_2^{\bullet -} \rightleftharpoons SO_2 + e^- \quad (4)$$

$$SO_2^{\bullet -} \cdots \text{solvent} \rightleftharpoons SO_2 + e^- \quad (5)$$

$$2SO_2^{\bullet -} \rightleftharpoons S_2O_4^{2-} \quad (6)$$

$$S_2O_4^{2-} \rightleftharpoons 2SO_2 + 2e^- \quad (7)$$

$$S_2O_4^{2-} \cdots \text{solvent} \rightleftharpoons 2SO_2 + 2e^- \quad (8)$$

Figures 5 shows cyclic voltammetry for the reduction of 25 to 500 parts-per-million (ppm) sulfur dioxide in (a) pure [C_2mim][NTf_2], (b) IL/poly(IL) 60/40 wt.% and (c) IL/poly(IL) 40/60 wt.% membranes on a Pt-TFE at a scan rate of 100 mV s^{-1}. The dashed lines represent the response in the absence of the analyte. Plots of peak current vs the square root of scan rate are linear (see Figure S3), suggesting that the sulfur dioxide reduction process is diffusion controlled in both the pure IL and in the membranes. Figure 5d shows the plots of peak current vs concentration and the corresponding linear calibration line for the three compositions. Similar to the case of oxygen, adding the poly(IL) does not appear to change the shape or number of the redox peaks, hence we expect that the electrochemical reaction mechanism is the same in the IL/poly(IL) membranes. The peak-to-peak separations (ΔE_p, see Table 2) appear to stay approximately the same or slightly decrease as the amount of poly(IL) increased, similar to the behaviour for oxygen, likely because of the different solvating nature of the pyrrolidinium compared to imidazolium. In the pure IL (Figure 5a), the potential is observed to shift quite significantly over the course of the experiment, which is a phenomenon we reported previously for oxygen and hydrogen gases in ILs with a Pt quasi-reference electrode [45]. However, the potential shifting is dramatically reduced in the IL/poly(IL) membranes, which is another promising feature of these robust membranes. The cause of the higher stability of the reference potential is believed to be because the IL/poly(IL) membrane is a solid and slows down the migration of electrogenerated products (formed at the working/counter electrodes) to the reference electrode.

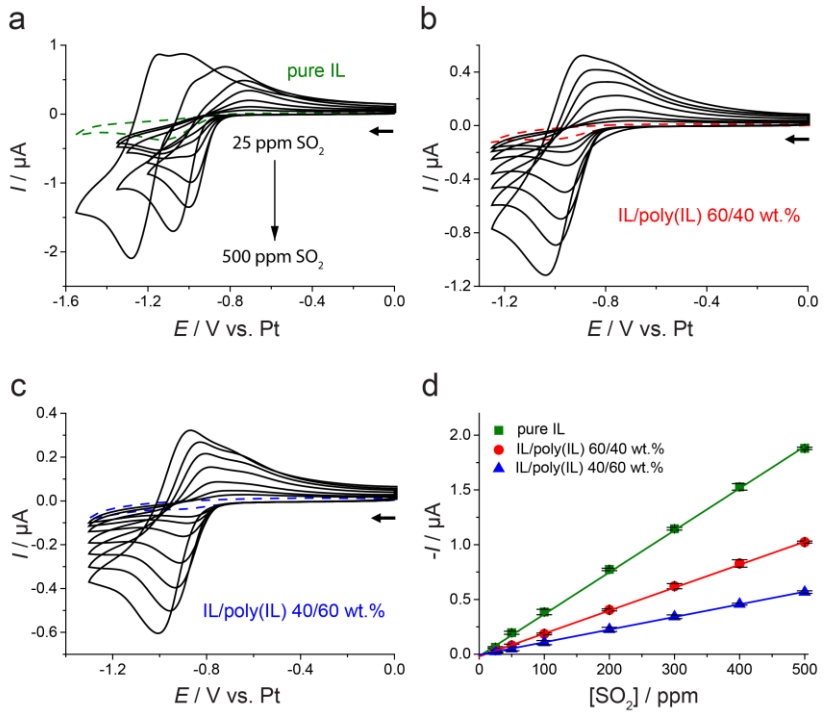

Figure 5. Cyclic voltammetry for electrochemical sulfur dioxide reduction at concentrations between 25 and 500 ppm in in (a) pure IL, (b) IL/poly(IL) 60/40 wt.% (c)) IL/poly(IL) 40/60 wt.% and (d) the respective baseline corrected calibration curves on a Pt-TFE (diameter = 1 mm). The dashed line represents the blank without sulfur dioxide at a scan rate of 100 mV s^{-1} and an overall flow rate of 500 mL min^{-1}. Error bars in (d) show one standard deviation for three runs on separate electrode devices.

The calibration graphs shown in Figure 5d are highly linear ($R^2 > 0.999$) for all three membrane compositions (see Table 2). The slopes of the lines decrease as the amount of poly(IL) increased in the membrane, which is consistent with the results for oxygen sensing. However, the LOD values improve with polymer addition, again because of the higher linearity of the calibration line (higher R^2 value in Table 2). The blank voltammograms shown as the dashed lines in Figure 5 show clearly that the impurity peak intrinsic to the imidazolium IL becomes smaller when the poly(IL) content increases, probably resulting in higher linearity of the measurement currents. This observation is highly encouraging because it should allow the detection of very low concentrations of gas without the complication of an overlaying impurity peak. It is noted that the limits of detection reported here are relatively high compared to literature values in ILs [41], however these can be significantly improved by studying lower concentrations, and this will be the focus of our future work.

3.3.3 Ammonia

The electrochemical ammonia (NH_3) oxidation mechanism has been studied in aprotic solvents by Schiffer at al. [46] as well as in RTILs [47]. It is believed to follow equations 9 to 11, with one chemically irreversible oxidation peak on the forward scan (equation 9), followed by two peaks on the reduction scan, corresponding to the reduction of the ammonium ion (equation 10) and the reduction of protons (equation 11) which are solvated by the IL anion [47].

$$4\,NH_3(g) \rightarrow 3\,NH_4^+ + \frac{1}{2}\,N_2(g) + 3\,e^- \quad (9)$$

$$NH_4^+ \rightleftharpoons NH_3 + H^+ \quad (10)$$

$$H^+ + e^- \rightarrow \frac{1}{2} H_2 \quad (11)$$

Figure 6 shows cyclic voltammetry responses for the oxidation of 20 to 500 ppm ammonia gas on a Pt-TFE taken at a scan rate of 100 mV s^{-1} and Figure 6d shows the respective background subtracted calibration curves. Generally, the peak shapes do not change significantly in the presence of the poly(IL), but because of the chemically irreversible nature of the oxidation peak, it is difficult to extract any data on the redox kinetics. Consistent with both O_2 and SO_2, the currents and sensitivities are lower with higher poly(IL) content, and diffusion control is observed from linear plots of peak current vs the square root of scan rate (see Figure S4). The calibration plots of peak current vs NH_3 concentration are linear ($R^2 > 0.995$) for all samples (see Table 3), and again, the LODs are not negatively affected by adding polymer. As mentioned above for the SO_2 analytical response, LODs for NH_3 are higher compared to that reported previously [42] because only higher concentration ranges for ammonia were tested to assess the behaviour of the poly(IL). Our future work will explore lower concentrations and the real analytical utility for ammonia sensing.

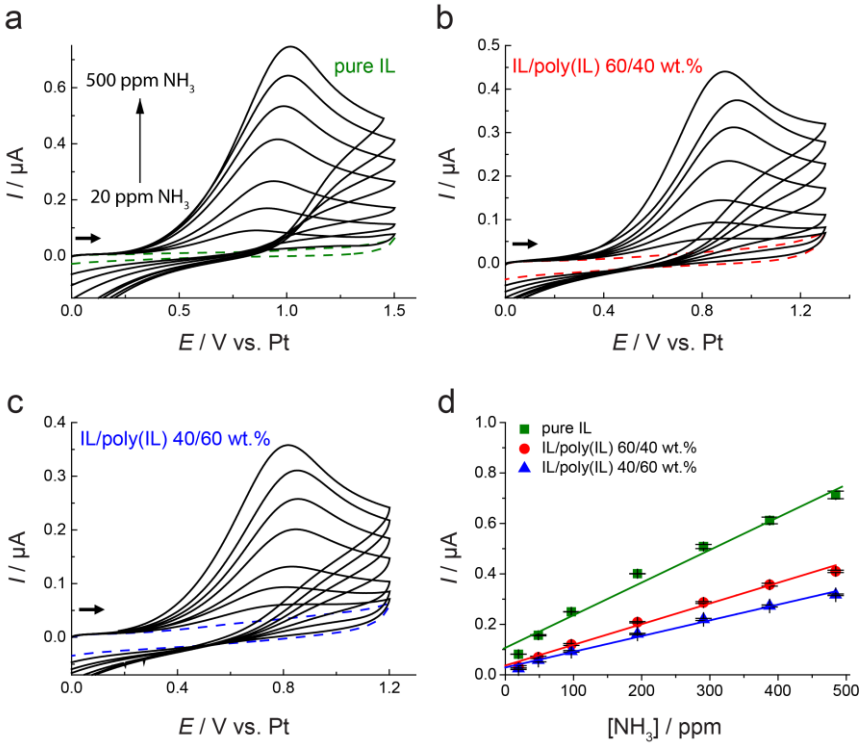

Figure 6. Cyclic voltammetry for electrochemical ammonia oxidation at concentrations between 20 and 500 ppm in (a) pure IL, (b) IL/poly(IL) 60/40 wt.% (c)) IL/poly(IL) 40/60 wt.% and (d) the respective baseline corrected calibration curves on a Pt-TFE (diameter = 1 mm). The dashed line represents the blank without ammonia at a scan rate of 100 mVs^{-1} and an overall flow rate of 500 mL min^{-1}. Error bars in (d) show one standard deviation for three runs on separate electrode devices.

Table 3. Summary of analytical parameters for electrochemical ammonia oxidation in the pure IL and IL/poly(IL) membranes (Pearson correlation coefficient (R^2), sensitivity, and calculated limit of detection (LOD)).

	Ammonia		
Sample	R^2	Sensitivity / nA/ppm	LOD / ppm
Pure IL	0.9883	1.25	81 ± 7
IL/poly(IL) 60/40 wt.%	0.9934	0.82	66 ± 4
IL/poly(IL) 40/60 wt.%	0.9933	0.62	65 ± 4

4. Conclusions

Ionic liquid/poly(ionic liquid) free-standing membranes have been explored for the first time as robust materials for 'membrane free' electrochemical (voltammetric) gas sensing. The blank responses in the absence of gas on both platinum and gold electrodes were first examined, with slightly wider potential windows observed when poly[DADMA][NTf_2] was added because of the higher stability of the pyrrolidinium cation compared to the imidazolium cation. While the peak-to-peak separations of the colabtocenium/cobaltocene redox couple increased slightly with higher poly(IL) content, it was the opposite case for the two chemically reversible gases, oxygen and sulfur dioxide. For O_2 and SO_2 reduction, the addition of the poly(IL) resulted in smaller peak-to-peak separations and faster electron transfer rate kinetics, probably because of the different solvation of the electrogenerated radical products by the pyrrolidinium moiety compared to imidazolium. For O_2, SO_2 and NH_3, highly linear calibration lines suggest that the IL/poly(IL) membranes can be used for highly robust voltametric/amperometric gas sensing. Additional benefits that the polymer brings include a cleaner blank response (leading to a lower LOD) and a more stable reference potential during measurements. In summary, poly(IL)s have much to offer in amperometric gas sensors, and future applications can be explored by tuning the chemical structure further to improve the analytical responses.

5. Acknowledgements

D.S.S. thanks the Australian Research Council for funding through a Future Fellowship (FT170100315). SD thanks Curtin University for a PhD scholarship. DM thanks the Agencia Española de Investigación (AEI) for funding through project PID2020-119026GB-I00. LCT is grateful to FCT (Fundação para a Ciência e a Tecnologia) in Portugal for her research contract under Scientific Employment Stimulus (2020.01555.CEECIND). Associate Laboratory for Green Chemistry – LAQV also acknowledge the financial support from FCT/MCTES (UIDB/50006/2020 and UIDP/50006/2020).

References

[1] J.R. Stetter, J. Li, Amperometric Gas Sensors - A Review, Chem. Rev., 108 (2008) 352-366.
[2] R. Baron, J. Saffell, Amperometric Gas Sensors as a Low Cost Emerging Technology Platform for Air Quality Monitoring Applications: A Review, ACS Sens., 2 (2017) 1553-1566.
[3] L. Xiong, R.G. Compton, Amperometric gas detection: A review, Int. J. Electrochem. Sci, 9 (2014) 7152-7181.
[4] J.L.C. Clark, R. Wolf, D. Granger, Z. Taylor, Continuous recording of blood oxygen tensions by polarography, Journal of Applied Physiology, 6 (1953) 189-193.
[5] M.C. Buzzeo, R.G. Evans, R.G. Compton, Non-Haloaluminate Room-Temperature Ionic Liquids in Electrochemistry—A Review, ChemPhysChem, 5 (2004) 1106-1120.
[6] M.C. Buzzeo, C. Hardacre, R.G. Compton, Use of Room Temperature Ionic Liquids in Gas Sensor Design, Anal. Chem., 76 (2004) 4583-4588.
[7] R. Toniolo, N. Dossi, A. Pizzariello, A.P. Doherty, G. Bontempelli, A Membrane Free Amperometric Gas Sensor Based on Room Temperature Ionic Liquids for the Selective Monitoring of NOx, Electroanalysis, 24 (2012) 865-871.
[8] D.S. Silvester, New innovations in ionic liquid–based miniaturised amperometric gas sensors, Curr. Opin. Electrochem., 15 (2019) 7-17.
[9] A. Rehman, X. Zeng, Methods and approaches of utilizing ionic liquids as gas sensing materials, RSC Adv., 5 (2015) 58371-58392.
[10] J. Lee, G. Du Plessis, D.W.M. Arrigan, D.S. Silvester, Towards imroving the robustness of electrochemical gas sensors: impact of PMMA addition on the sensing of oxygen in an ionic liquid, Anal. Methods, 7 (2015) 7327-7335.
[11] J. Lee, G. Hussain, N. López-Salas, D.R. MacFarlane, D.S. Silvester, Thin films of poly (vinylidene fluoride-co-hexafluoropropylene)-ionic liquid mixtures as amperometric gas sensing materials for oxygen and ammonia, Analyst, 145 (2020) 1915-1924.
[12] P. Kuberský, J. Altšmíd, A. Hamáček, S. Nešpůrek, O. Zmeškal, An Electrochemical NO_2 Sensor Based on Ionic Liquid: Influence of the Morphology of the Polymer Electrolyte on Sensor Sensitivity, Sensors, 15 (2015) 28421-28434.
[13] M. Nádherná, F. Opekar, J. Reiter, Ionic liquid–polymer electrolyte for amperometric solid-state NO_2 sensor, Electrochim. Acta, 56 (2011) 5650-5655.
[14] D. Mecerreyes, Polymeric ionic liquids: Broadening the properties and applications of polyelectrolytes, Prog. Polym. Sci., 36 (2011) 1629-1648.
[15] J. Qin, J. Guo, Q. Xu, Z. Zheng, H. Mao, F. Yan, Synthesis of Pyrrolidinium-Type Poly(ionic liquid) Membranes for Antibacterial Applications, ACS Appl. Mater. Interfaces, 9 (2017) 10504-10511.
[16] C. Pozo-Gonzalo, R. Marcilla, M. Salsamendi, D. Mecerreyes, J.A. Pomposo, J. Rodríguez, H.J. Bolink, PEDOT:Poly(1-vinyl-3-ethylimidazolium) dispersions as alternative materials for optoelectronic devices, J. Polym. Sci. Part A Polym. Chem., 46 (2008) 3150-3154.
[17] T.K. Kim, M. Suh, S.J. Kwon, T.H. Lee, J.E. Kim, Y.J. Lee, J.H. Kim, M.P. Hong, K.S. Suh, Poly(3,4-ethylenedioxythiophene) Derived from Poly(ionic liquid) for the Use as Hole-Injecting Material in Organic Light-Emitting Diodes, Macromol. Rapid Commun., 30 (2009) 1477-1482.
[18] S.-Y. Zhang, Q. Zhuang, M. Zhang, H. Wang, Z. Gao, J.-K. Sun, J. Yuan, Poly(ionic liquid) composites, Chem. Soc. Rev., 49 (2020) 1726-1755.
[19] H. Fang, S. Sun, P. Liao, Y. Hu, J. Zhang, Gold nanoparticles confined in imidazolium-based porous organic polymers to assemble a microfluidic reactor: controllable growth and enhanced catalytic activity, J. Mater. Chem. A, 6 (2018) 2115-2121.
[20] X. Li, Z. Zhang, S. Li, K. Yang, L. Yang, Polymeric ionic liquid–ionic plastic crystal all-solid-state electrolytes for wide operating temperature range lithium metal batteries, J. Mater. Chem. A, 5 (2017) 21362-21369.
[21] S. Zulfiqar, M.I. Sarwar, D. Mecerreyes, Polymeric ionic liquids for CO2 capture and separation: potential, progress and challenges, Polym. Chem., 6 (2015) 6435-6451.
[22] L.C. Tomé, I.M. Marrucho, Ionic liquid-based materials: a platform to design engineered CO_2 separation membranes, Chem. Soc. Rev., 45 (2016) 2785-2824.

[23] Z. Wang, Y. Si, C. Zhao, D. Yu, W. Wang, G. Sun, Flexible and Washable Poly(Ionic Liquid) Nanofibrous Membrane with Moisture Proof Pressure Sensing for Real-Life Wearable Electronics, ACS Appl. Mater. Interfaces, 11 (2019) 27200-27209.
[24] W. Jeffrey Horne, M.A. Andrews, M.S. Shannon, K.L. Terrill, J.D. Moon, S.S. Hayward, J.E. Bara, Effect of branched and cycloalkyl functionalities on CO2 separation performance of poly(IL) membranes, Sep. Purif. Technol., 155 (2015) 89-95.
[25] J.E. Bara, S. Lessmann, C.J. Gabriel, E.S. Hatakeyama, R.D. Noble, D.L. Gin, Synthesis and Performance of Polymerizable Room-Temperature Ionic Liquids as Gas Separation Membranes, Ind. Eng. Chem. Res., 46 (2007) 5397-5404.
[26] L.C. Tomé, D.C. Guerreiro, R.M. Teodoro, V.D. Alves, I.M. Marrucho, Effect of polymer molecular weight on the physical properties and CO_2/N_2 separation of pyrrolidinium-based poly (ionic liquid) membranes, J. Membr. Sci., 549 (2018) 267-274.
[27] R. Jamil, L.C. Tomé, D. Mecerreyes, D.S. Silvester, Emerging Ionic Polymers for CO2 Conversion to Cyclic Carbonates: An Overview of Recent Developments, Aust. J. Chem., 74 (2021) 767-777.
[28] Q. Zhao, M. Yin, A.P. Zhang, S. Prescher, M. Antonietti, J. Yuan, Hierarchically Structured Nanoporous Poly(Ionic Liquid) Membranes: Facile Preparation and Application in Fiber-Optic pH Sensing, J. Am. Chem. Soc., 135 (2013) 5549-5552.
[29] J. Huang, C. Tao, Q. An, W. Zhang, Y. Wu, X. Li, D. Shen, G. Li, 3D-ordered macroporous poly(ionic liquid) films as multifunctional materials, Chem. Commun., 46 (2010) 967-969.
[30] S. Lee, B.S. Ringstrand, D.A. Stone, M.A. Firestone, Electrochemical Activity of Glucose Oxidase on a Poly(ionic liquid)–Au Nanoparticle Composite, ACS Appl. Mater. Interfaces, 4 (2012) 2311-2317.
[31] C. Willa, J. Yuan, M. Niederberger, D. Koziej, When Nanoparticles Meet Poly(Ionic Liquid)s: Chemoresistive CO_2 Sensing at Room Temperature, Adv. Funct. Mater., 25 (2015) 2537-2542.
[32] Y. Li, G. Li, X. Wang, Z. Zhu, H. Ma, T. Zhang, J. Jin, Poly(ionic liquid)-wrapped single-walled carbon nanotubes for sub-ppb detection of CO2, Chem. Commun., 48 (2012) 8222-8224.
[33] L.C. Tomé, D. Mecerreyes, C.S.R. Freire, L.P.N. Rebelo, I.M. Marrucho, Pyrrolidinium-based polymeric ionic liquid materials: New perspectives for CO_2 separation membranes, J. Membr. Sci., 428 (2013) 260-266.
[34] J. Lee, K. Murugappan, D.W.M. Arrigan, D.S. Silvester, Oxygen reduction voltammetry on platinum macrodisk and screen-printed electrodes in ionic liquids: Reaction of the electrogenerated superoxide species with compounds used in the paste of Pt screen-printed electrodes?, Electrochim. Acta, 101 (2013) 158-168.
[35] S. Doblinger, T.J. Donati, D.S. Silvester, Effect of Humidity and Impurities on the Electrochemical Window of Ionic Liquids and Its Implications for Electroanalysis, J. Phys. Chem. C, 124 (2020) 20309-20319.
[36] A.-L. Pont, R. Marcilla, I. De Meatza, H. Grande, D. Mecerreyes, Pyrrolidinium-based polymeric ionic liquids as mechanically and electrochemically stable polymer electrolytes, J. Power Sources, 188 (2009) 558-563.
[37] S.K. Sukardi, J. Zhang, I. Burgar, M.D. Horne, A.F. Hollenkamp, D.R. MacFarlane, A.M. Bond, Prospects for a widely applicable reference potential scale in ionic liquids based on ideal reversible reduction of the cobaltocenium cation, Electrochem. Commun., 10 (2008) 250-254.
[38] C. Fu, L. Aldous, E.J.F. Dickinson, N.S.A. Manan, R.G. Compton, Volatilisation of ferrocene from ionic liquids: kinetics and mechanism, Chem. Commun., 47 (2011) 7083-7085.
[39] C. Lagrost, L. Preda, E. Volanschi, P. Hapiot, Heterogeneous electron-transfer kinetics of nitro compounds in room-temperature ionic liquids, J. Electroanal. Chem., 585 (2005) 1-7.
[40] A. Lewandowski, L. Waligora, M. Galinski, Electrochemical Behavior of Cobaltocene in Ionic Liquids, J. Solution Chem., 42 (2013) 251-262.
[41] S. Doblinger, J. Lee, Z. Gurnah, D.S. Silvester, Detection of sulfur dioxide at low parts-per-million concentrations using low-cost planar electrodes with ionic liquid electrolytes, Anal. Chim. Acta, 1124 (2020) 156-165.
[42] G. Hussain, D.S. Silvester, Detection of sub-ppm Concentrations of Ammonia in an Ionic Liquid: Enhanced Current Density Using “Filled” Recessed Microarrays, Anal. Chem., 88 (2016) 12453-12460.
[43] M. Hayyan, F.S. Mjalli, M.A. Hashim, I.M. AlNashef, X.M. Tan, Electrochemical reduction of dioxygen in Bis(trifluoromethylsulfonyl)imide based ionic liquids, J. Electroanal. Chem., 657 (2011) 150-157.
[44] L.E. Barrosse-Antle, D.S. Silvester, L. Aldous, C. Hardacre, R.G. Compton, Electroreduction of Sulfur Dioxide in Some Room-Temperature Ionic Liquids, J. Phys. Chem. C, 112 (2008) 3398-3404.

[45] J. Wandt, J. Lee, D.W.M. Arrigan, D.S. Silvester, A lithium iron phosphate reference electrode for ionic liquid electrolytes, Electrochem. Commun., 93 (2018) 148-151.
[46] Z. Schiffer, N. Lazouski, N. Corbin, K. Manthiram, Rate-Determining Step and Mechanistic Understanding of Electrochemical Ammonia Oxidation in a Non-Aqueous Electrolyte, 2019 North American Catalysis Society Meeting, NAM, 2019.
[47] X. Ji, D.S. Silvester, L. Aldous, C. Hardacre, R.G. Compton, Mechanistic Studies of the Electro-oxidation Pathway of Ammonia in Several Room-Temperature Ionic Liquids, J. Phys. Chem. C, 111 (2007) 9562-9572.